Tutorial Vol. 41, No. 12 / December 2024 / Journal of the Optical Society of America A 2361

Journal of the Optical Society of America A

OPTICS, IMAGE SCIENCE, AND VISION

Fourier-optics imaging analysis with ABCD matrices: tutorial

JAMES R. FIENUP

Institute of Optics, University of Rochester, Rochester, New York, USA (fienup@optics.rochester.edu)

Received 8 August 2024; revised 24 October 2024; accepted 24 October 2024; posted 25 October 2024; published 12 November 2024

The use of ABCD (ray-transfer) matrices to analyze wave propagation through paraxial optical systems, with emphasis on imaging systems, is described. It is shown how to find the image, Fourier transform, and exit pupil planes. Different forms of the propagation integrals are given. The propagation integral for an imaging system, which includes an aperture stop, is derived. The relationships between the aperture stop and the exit pupil and the impulse response of a paraxial imaging system are derived.

https://doi.org/10.1364/JOSAA.538781

1. INTRODUCTION

ABCD (ray-transfer) matrices were used in paraxial geometrical optics to simplify calculations of the first-order properties of systems in the context of rays. In 1970, Collins [1] showed how to use ABCD matrices to calculate the propagation of paraxial optical fields through complicated optical systems using a single propagation integral. This contrasts with the laborious process of numerically propagating through each optical element and over the distances between successive optical elements. Hence, Collins's ABCD propagation is highly advantageous for analyzing the propagation through any paraxial, symmetric optical system except for the simplest free-space propagation calculations. In this paper, we are primarily concerned with the propagation integrals for imaging, in which case some interesting aspects emerge. Although the use of ABCD matrices for optical propagations has long appeared in Siegman's *Lasers* [2], it is curiously absent from other popular textbooks [3,4] and appeared only in the most recent 2017 edition of Goodman's *Introduction to Fourier Optics* [5]. The power of the approach makes it worthy of greater notice, and its use for imaging has been particularly hidden from sight.

In this paper, after briefly defining the key ABCD matrices, we review the propagation integral and then show under what circumstances it reduces to a Fourier transforming equation and to an imaging equation, and how it can predict the locations of both Fourier planes and image planes. We derive an alternative, convolutional form of ABCD propagation, which is particularly useful for imaging. This convolutional form is usually most efficiently computed with two Fourier transforms (FTs) for a general ABCD system, so we refer to it as the double-FT version of ABCD propagation. Next, we introduce an aperture stop into a multi-element system and derive the impulse response of the system, first in terms of the aperture stop and then in terms of the exit pupil of the system, which is the image of the aperture stop, as seen from image space.

What is said in this paper about ABCD propagation integrals can be readily applied to propagations by fractional Fourier transforms [6] and linear canonical transforms [7], since they are special cases of ABCD propagation integrals using different parameterizations [8].

For the sake of simplicity, in this paper we restrict our attention to symmetric optical systems, although anamorphic optics can be handled as well [1].

2. ABCD RAY-TRANSFER MATRICES

For a rotationally symmetric paraxial system, a ray of light in the $y-z$ plane, at a particular axial distance z, is specified by its ray height y and its reduced angle $\hat{\theta}$, which is the physical ray angle θ times the index of refraction of the medium. Use of the reduced, rather than the actual, angles simplifies the math [2]. Furthermore, in the paraxial approximation, we consider ray slopes and angles to be the same thing. ABCD matrices encapsulate a pair of linear equations for y and $\hat{\theta}$ of a ray exiting a system in terms of y and $\hat{\theta}$ of the corresponding ray entering the system. In the paraxial approximation, a small angle ($\ll 1$ rad) is assumed, with the angle, in radians, being equal to the tangent of the angle and the sine of the angle. Following ([5], Appendix B), and as illustrated in Fig. 1, if a ray with height y_1 and reduced angle $\hat{\theta}_1$ enters a system, then the ray with height y_2 and reduced angle $\hat{\theta}_2$ that exits the system is given by

$$y_2 = Ay_1 + B\hat{\theta}_1$$

$$\hat{\theta}_2 = Cy_1 + D\hat{\theta}_1, \tag{1}$$

or, in matrix form,

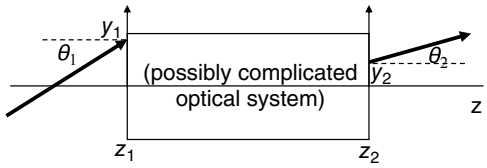

Fig. 1. Rays into and out from an ABCD system.

$$\begin{bmatrix} y_2 \\ \hat{\theta}_2 \end{bmatrix} = \begin{bmatrix} A & B \\ C & D \end{bmatrix} \begin{bmatrix} y_1 \\ \hat{\theta}_1 \end{bmatrix}, \tag{2}$$

where A, B, C, and D are the coefficients of the ray-transfer matrix, also referred to as the ABCD matrix.

For simplicity, we employ only the two most basic ABCD matrices. For propagating an axial distance z in a medium with a constant refractive index n, the matrix is

$$M_z = \begin{bmatrix} A_z & B_z \\ C_z & D_z \end{bmatrix} = \begin{bmatrix} 1 & z/n \\ 0 & 1 \end{bmatrix}, \tag{3}$$

and for propagating through a thin lens of focal length f, embedded in a medium with refractive index n_1, the matrix is

$$M_f = \begin{bmatrix} A_f & B_f \\ C_f & D_f \end{bmatrix} = \begin{bmatrix} 1 & 0 \\ \frac{-n_1}{f} & 1 \end{bmatrix}. \tag{4}$$

If mirrors are employed instead of lenses, then this equation holds for the unfolded version of the system with the mirrors. The matrix for a system, consisting of a combination of a sequence of lenses and spacings, is given by the matrix product of the basic 2×2 matrices for the individual lenses and spacings. From the two equations above it is readily seen that the determinant of these two basic matrices is unity. Hence, the matrix for a system made up of an arbitrary combination of them has a determinant that is unity:

$$AD - BC = 1, \tag{5}$$

which is generally true for ABCD matrices. Hence, each matrix consisting of four values is completely specified by any three of them, and the fourth value can be computed from the other three. Siegman ([2], Table 15.1) provides matrices for a few other paraxial optical elements.

3. SINGLE-FOURIER TRANSFORM ABCD PROPAGATION INTEGRAL

As derived by Collins [1,2,5], given the ABCD matrix for an arbitrary complicated ABCD paraxial system, the field U_2 at the output plane of the system is given in terms of the field U_1 at the input plane of the system by, using Goodman's notation [5],

$$U_2(x, y) = \frac{e^{ikL_0}}{i\lambda B} \iint_{-\infty}^{\infty} \mathrm{d}\xi \,\mathrm{d}\eta \; U_1(\xi, \eta) \times \exp\left\{ \frac{i\pi}{\lambda B} \left[A\left(\xi^2 + \eta^2\right) - 2(\xi x + \eta y) + D\left(x^2 + y^2\right) \right] \right\}, \tag{6}$$

$$U_2(x, y) = \frac{e^{ikL_0}}{i\lambda B} \exp\left[\frac{i\pi D}{\lambda B} \left(x^2 + y^2\right) \right] \times \iint_{-\infty}^{\infty} \mathrm{d}\xi \,\mathrm{d}\eta \left\{ U_1(\xi, \eta) \exp\left[\frac{i\pi A}{\lambda B} \left(\xi^2 + \eta^2\right) \right] \right\} \times \exp\left[\frac{-i2\pi}{\lambda B} (\xi x + \eta y) \right], \tag{7}$$

where L_0 is the optical path length through the center of the system along the optical axis, k is the wave number, and λ is the wavelength (assumed to be monochromatic). The second form above emphasizes that, aside from one quadratic-phase exponential factor inside the integral and a second outside the integral, this paraxial propagation integral includes, at its core, a Fourier transform. In this paper, we refer to this as the single-FT version. Note that for free-space propagation through a medium with unity index of refraction, $A = D = 1$, and $B = z$, the propagation distance, and the integral becomes the familiar Fresnel transform,

$$\begin{aligned} U_2(x, y) &= \frac{e^{ikz}}{i\lambda z} \iint_{-\infty}^{\infty} \mathrm{d}\xi \,\mathrm{d}\eta \; U_1(\xi, \eta) \times \exp\left\{ \frac{i\pi}{\lambda z} \left[(x - \xi)^2 + (y - \eta)^2 \right] \right\} \\ &= \frac{e^{ikz}}{i\lambda z} \exp\left[\frac{i\pi}{\lambda z} \left(x^2 + y^2\right) \right] \times \iint_{-\infty}^{\infty} \mathrm{d}\xi \,\mathrm{d}\eta \left\{ U_1(\xi, \eta) \exp\left[\frac{i\pi}{\lambda z} \left(\xi^2 + \eta^2\right) \right] \right\} \times \exp\left[\frac{-i2\pi}{\lambda z} (\xi x + \eta y) \right]. \end{aligned} \tag{8}$$

In this paper, we use the $e^{-i\omega t}$ sign convention, that is, the phase becomes larger with longer propagation distances.

It is also possible for the ABCD coefficients to be complex valued [9,10]. If one were to have a Gaussian amplitude transmittance (like an apodization) within the system, then its ABCD matrix is similar to that of the transmittance of a lens, but with a pure imaginary C component. That changes a quadratic-phase exponential into a Gaussian amplitude function. In this paper, we will restrict our attention to real-valued ABCD coefficients.

4. FOURIER TRANSFORMING

When $A = 0$, the quadratic-phase exponential within the integral of Eq. (7) becomes unity, and the integral becomes an optical Fourier transform of the input field, with output spatial frequencies $(f_x, f_y) = (x/\lambda B, y/\lambda B)$. Note that we need not worry about B being equal to zero when $A = 0$ because that is prevented by Eq. (5). A characteristic of this Fourier transform is that a bundle of parallel rays (i.e., a tilted plane wave) entering the system focuses to a point in the output plane of the system.

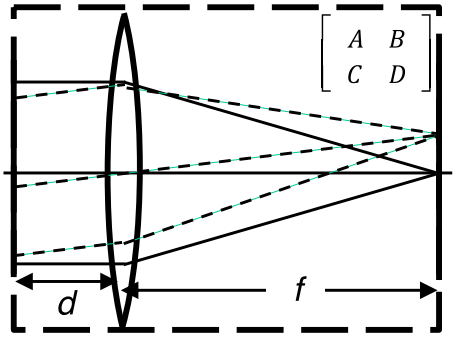

Fig. 2. Fourier transforming when $A=0$, $D\neq 0$. The box indicates the left and right edges of the system.

This agrees with the fact that the Fourier transform of a constant or of a linear-phase function (a plane wave) is a Dirac delta function. An example of such a system is one starting at a distance d before a thin lens of focal length f and ending in the plane at a distance $z=f$ beyond the lens (i.e., in the back focal plane of the lens), as shown in Fig. 2. The ABCD matrix for this system is given by

$$\begin{bmatrix} 1 & f \\ 0 & 1 \end{bmatrix}\begin{bmatrix} 1 & 0 \\ -1/f & 1 \end{bmatrix}\begin{bmatrix} 1 & d \\ 0 & 1 \end{bmatrix}=\begin{bmatrix} 0 & f \\ -1/f & 1-d/f \end{bmatrix}. \quad \textbf{(9)}$$

The Fourier relationship is also seen by examining Eq. (1) which, with $A=0$, yields $y_2=B\hat{\theta}_1=f\hat{\theta}_1$ in this case, which indicates that the output ray height is independent of the input ray height and is proportional to the input ray angle. This Fourier transform has an additional quadratic phase term outside the integral, proportional to $D/B=(1-d/f)/f$, unless $d=f$ as well, in which case the external quadratic-phase factor disappears ([5], Ch. 6). This external quadratic-phase term means that a point source (Dirac delta function) in the input plane will result in a quadratic-phase factor in the output plane, which is the paraxial approximation of a spherical wave coming from a distance $B/D=f^2/(f-d)$ before the output plane (or focusing to a distance $|B/D|$ after the output plane if B/D has a negative value).

If $D=0$ as well as $A=0$, which is the special case in Fig. 2 for $d=f$, and illustrated in Fig. 3, the quadratic phase exponentials both inside and outside the propagation integral vanish, and we have just a simple Fourier transform, aside from a multiplicative constant. Then Eq. (1) yields $\hat{\theta}_2=Cy_1$, which indicates that the output ray angle is independent of the input ray angle and depends only on the input ray height, as shown in Fig. 3(b). As a result, a point source in the input plane results in a tilted plane wave in the output.

5. DOUBLE-FOURIER TRANSFORM/ CONVOLUTION/TRANSFER-FUNCTION VERSION

Understanding imaging from Eq. (1) is straightforward: for $B=0$, $y_2=Ay_1$, and the output ray height is independent of the input ray angle and is simply proportional to the input ray height, with proportionality constant A. That is, the output is an image of the input with magnification A. Obtaining an imaging equation from Eq. (6) or (7) requires more finesse. This

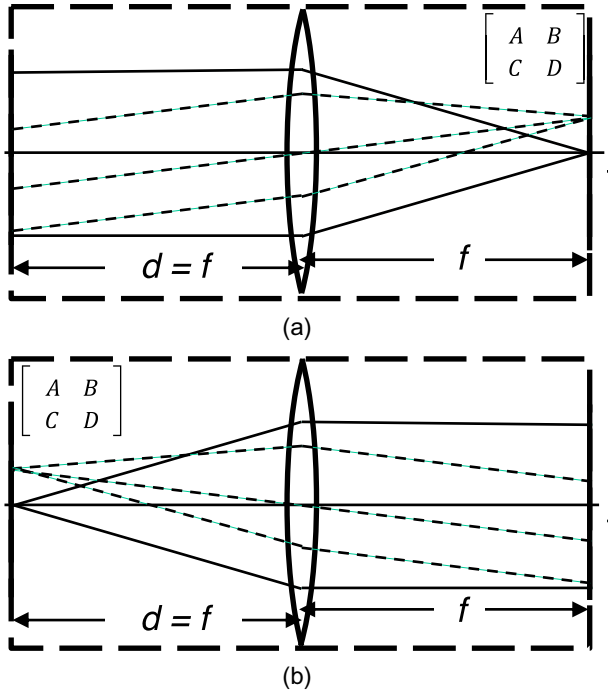

Fig. 3. Fourier transforming when $A=0$, $D=0$. (a) Plane waves focus to points. (b) Points expand to plane waves.

is aided by converting the general single-FT ABCD propagation integral into a convolution, which can be computed using a Fourier-domain transfer function. To achieve this, we complete the squares of the exponentials inside the integral, which involves bringing an exponential outside the integral, giving

$$\begin{aligned} U_2(x,y)=&\frac{e^{ikL_0}}{i\lambda B}\exp\left[\frac{i\pi}{\lambda B}\left(D-A^{-1}\right)\left(x^2+y^2\right)\right]\\ &\times\iint_{-\infty}^{\infty}U_1(\xi,\eta)\\ &\times\exp\left\{\frac{i\pi A}{\lambda B}\left[(\xi-x/A)^2+(\eta-y/A)^2\right]\right\}\mathrm{d}\xi\,\mathrm{d}\eta. \end{aligned} \quad \textbf{(10)}$$

The integral can now be recognized as a convolution of the input field with a quadratic-phase exponential. Using $(D-A^{-1})/B=C/A$ from Eq. (5), we can rewrite this as

$$\begin{aligned} U_2(x,y)=&\frac{e^{ikL_0}}{A}\exp\left[\frac{i\pi C}{\lambda A}\left(x^2+y^2\right)\right]\Bigg\{U_1(\xi,\eta)\\ &*\frac{A}{i\lambda B}\exp\left[\frac{i\pi A}{\lambda B}\left(\xi^2+\eta^2\right)\right]\Bigg\}_{\substack{\xi=x/A\\ \eta=y/A}}, \end{aligned} \quad \textbf{(11)}$$

where $*$ denotes convolution. In this form, we see that a general ABCD propagation can be expressed as a convolution with the ABCD impulse response given by the expression to the right of the $*$ symbol above, but then, in addition, multiplying the resulting convolution by the constant and the quadratic-phase exponential in front of the convolution integral. Because one can compute a convolution of two functions by Fourier transforming each function, taking the product of their Fourier

transforms and inverse Fourier transforming, we can write

$$U_2(x,y)=\frac{e^{ikL_0}}{A}\exp\left[\frac{i\pi C}{\lambda A}\left(x^2+y^2\right)\right]\left\{\mathcal{F}^{-1}\left\{\mathcal{F}[U_1(\xi,\eta)]\times\exp\left[\frac{-i\pi\lambda B}{A}\left(f_x^2+f_y^2\right)\right]\right\}\right\}\Big|_{\substack{\xi=x/A\\ \eta=y/A}}, \tag{12}$$

where $\mathcal{F}$ denotes a forward Fourier transform,

$$\mathcal{F}[U_1(\xi,\eta)]=\iint_{-\infty}^{\infty}U_1(\xi,\eta)\exp\left[-i2\pi\left(f_x\xi+f_y\eta\right)\right]\mathrm{d}\xi\,\mathrm{d}\eta, \tag{13}$$

and where

$$\mathcal{F}\left\{\frac{A}{i\lambda B}\exp\left[\frac{i\pi A}{\lambda B}\left(\xi^2+\eta^2\right)\right]\right\}=\exp\left[\frac{-i\pi\lambda B}{A}\left(f_x^2+f_y^2\right)\right]. \tag{14}$$

Equations (11) and (12) are the alternative ABCD propagation integrals in terms of convolution with a quadratic-phase exponential impulse response and in terms of a quadratic-phase exponential Fourier-domain transfer function, respectively, irrespective of whether imaging is performed. Equation (14) shows the Fourier relationship between the impulse response and the Fourier-domain transfer function. In this paper, we refer to Eq. (12) as the double-FT version of the ABCD propagation integral.

6. IMAGING WITH NO APERTURE STOP

For the special case of an imaging system, $B=0$ [5], which appears to be problematic with B appearing in two denominators in the convolution of Eq. (11). However, inspecting the right hand side of Eq. (14), we see that as B approaches zero, the right hand side of Eq. (14) approaches unity, which is well behaved, and the Fourier transform of unity is the Dirac delta function. Hence, when $B=0$, U_1 in Eq. (11) is convolved with a Dirac delta function as the impulse response, which convolution gives a perfect magnified version of the input as the output. Looking at it another way, replacing the exponential inside the Fourier transform of Eq. (12) with unity, one performs a forward then an inverse Fourier transform on U_1, getting back the same thing. But on account of the substitution $\xi=x/A$ and $\eta=y/A$, the output for $B=0$, is the image

$$U_2(x,y)=\frac{e^{ikL_0}}{A}\exp\left[\frac{i\pi C\left(x^2+y^2\right)}{\lambda A}\right]U_1\left(\frac{x}{A},\frac{y}{A}\right), \tag{15}$$

which we see is not only a perfect magnified image of the input field, with magnification $M=A$, but it also has an additional quadratic phase term. An extra quadratic phase exponential (which is a wavefront curvature term) is the norm for the imaging of optical fields, although it is often ignored {[5], after Eq. (6–34)}. It is important to keep these external quadratic-phase terms when numerically or analytically propagating optical fields when the phases of those fields matter, as would be the case if that field is interfered with itself or another field or if further propagation of the field is needed.

As an example, consider the single-thin-lens imaging system illustrated in Fig. 4. For arbitrary z_1 and z_2, the ABCD matrix for this system is

$$\begin{pmatrix}1 & z_2\\ 0 & 1\end{pmatrix}\begin{pmatrix}1 & 0\\ -\frac{1}{f} & 1\end{pmatrix}\begin{pmatrix}1 & z_1\\ 0 & 1\end{pmatrix}=\begin{pmatrix}1-\frac{z_2}{f} & z_1+z_2-\frac{z_1z_2}{f}\\ -\frac{1}{f} & -\frac{z_1}{f}+1\end{pmatrix}. \tag{16}$$

Given that $B=0$ for an imaging system, setting the B coefficient in the right-hand side of Eq. (16) to zero and solving for z_2 in terms of z_1 and f, we obtain the imaging condition,

$$z_2=\left(\frac{1}{f}-\frac{1}{z_1}\right)^{-1}=\frac{z_1f}{z_1-f}. \tag{17}$$

This is the well-known lens law. The magnification M, given by the A coefficient, is

$$M=A=1-\frac{z_2}{f}=-\frac{z_2}{z_1}, \tag{18}$$

where we used the expression for f obtained by solving Eq. (17) for f,

$f=(z_1^{-1}+z_2^{-1})^{-1}=z_1z_2/(z_1+z_2)$. The quadratic-phase factor associated with the image given by Eq. (15) has the coefficient

$$\frac{C}{A}=\frac{-1/f}{-z_2/z_1}=-\frac{1}{Mf}. \tag{19}$$

With some algebra, this can be shown to be identical to the product of the two terms under Eq. (6–33) in [5], including the substitution of Eq. (6–35) in [5]. As the magnification given by Eq. (18) is negative for imaging with a single positive thin lens, that quadratic-phase factor in the image is equivalent to one from a point source at a distance $-Mf=|Mf|$ before the lens. For a general ABCD imaging system, the quadratic-phase factor can be that from a point source either before or after the image plane depending on the sign of C/A.

Not all imaging systems have additional quadratic phase factors, the most well-known being the $4-f$ system. This is just a concatenation of two systems, each form is shown in Fig. 3. Each of these has the ABCD matrix given by Eq. (9) for the special case of $d=f$, so the entire $4-f$ imaging system has the matrix

$$\begin{bmatrix}0 & f\\ -1/f & 0\end{bmatrix}\begin{bmatrix}0 & f\\ -1/f & 0\end{bmatrix}=\begin{bmatrix}-1 & 0\\ 0 & -1\end{bmatrix}. \tag{20}$$

From this we see that it is an imaging system, because its $B=0$, has magnification $A=-1$, and has a quadratic phase proportional to $C/A=0$, that is, no quadratic-phase factor.

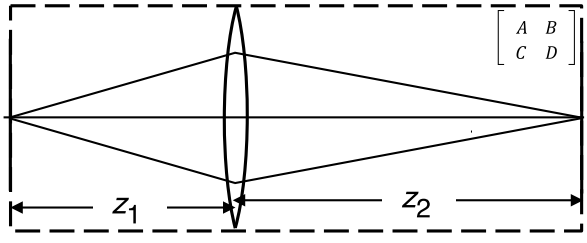

Fig. 4. Single thin lens imaging system having an object plane at distance z_1 before the lens of focal length f and the image plane at distance z_2 after the lens.

7. IMAGING WITH AN APERTURE STOP

The preceding material in this paper has been known, but it implicitly assumes lenses of infinite diameter or fields that are negligible beyond the diameter of the lenses and aperture stops. This section presents an analysis of a general ABCD imaging system containing an aperture stop, which was not found in the general case in the literature. We wish to derive the well-known result that the impulse response of an imaging system is a scaled version of the Fourier transform of the exit pupil of the system. Therefore, one must derive both the impulse response and the location and magnification of the exit pupil.

First, consider a general (imaging or non-imaging) ABCD system containing an aperture stop within the system. When there is a significant aperture stop, then the input field from the object must first be propagated to the plane of the aperture stop, then multiplied by the stop (pupil) field (amplitude) transmittance function P in that plane, and finally propagated from there to the output plane, as illustrated in Fig. 5. [While making revisions to this paper, I found that Collins proposed this same approach in a presentation at an OSA Annual Meeting [11], but the reference gives no details, and according to Google Scholar it has had no citations].

The derivation can be performed in two ways. The first, as described above, is to propagate the input field U_1, perform the multiplication, and then perform the second propagation. The second is to follow the approach in [5] (Sect. 6.3) of propagating a field from a point source in the input plane to the output plane, having gone through the aperture stop, and identifying the resultant field as the (coherent) impulse response of the system. Here, we employ the second approach.

As in {[5], Eq. (6–28)]}, a system linear in optical field can be expressed as the superposition integral

$$U_3(u,v)=\iint_{-\infty}^{\infty} h(u,v;\xi,\eta)U_1(\xi,\eta)\,\mathrm{d}\xi\mathrm{d}\eta, \tag{21}$$

where $h(u,v;\xi,\eta)$ is the impulse response of the system, the field at a point (u,v) in the output plane that arises from a point source (Dirac delta function) at location (ξ,η) in the input plane.

The point source $U_1(\xi,\eta)=\delta(\xi-\xi_o,\eta-\eta_o)$ located at point (ξ_o,η_o) in the input plane, inserted into the Eq. (7) for the first subsystem, yields a field impinging on the aperture stop,

$$\begin{aligned}U_2(x,y;\xi_o,\eta_o)=&\frac{e^{ikL_{01}}}{i\lambda B_1}\exp\left[\frac{i\pi D_1}{\lambda B_1}\left(x^2+y^2\right)\right]\\&\times\exp\left[\frac{i\pi A_1}{\lambda B_1}\left(\xi_o^2+\eta_o^2\right)\right]\\&\times\exp\left[\frac{-i2\pi}{\lambda B_1}\left(\xi_o x+\eta_o y\right)\right],\end{aligned} \tag{22}$$

where L_{01} is the axial optical path. We used the sifting property of the delta function. Here, $U_2(x,y;\xi_o,\eta_o)$ is the specific field in the (x,y) plane due to a point source at (ξ_o,η_o) in the input plane. The field immediately after the pupil is $U_2'(x,y;\xi_o,\eta_o)=U_2(x,y;\xi_o,\eta_o)P(x,y)$. The field in the output plane is given by Eq. (7) again but substituting $U_3(u,v;\xi_o,\eta_o)$ for $U_2(x,y;\xi_o,\eta_o)$, $U_2'(x,y;\xi_o,\eta_o)$ for $U_1(\xi,\eta)$, and using matrix coefficient subscripts 2. Inserting the expression for $U_2'(x,y;\xi_o,\eta_o)$, we obtain the 4D (which can in general be space-variant) impulse response

$$\begin{aligned}h(u,v;\xi_o,\eta_o)=&U_3(u,v;\xi_o,\eta_o)\\=&\frac{e^{ikL_0}}{i\lambda B_2}\frac{1}{i\lambda B_1}\exp\left[\frac{i\pi D_2}{\lambda B_2}\left(u^2+v^2\right)\right]\\&\times\exp\left[\frac{i\pi A_1}{\lambda B_1}\left(\xi_o^2+\eta_o^2\right)\right]\\&\times\iint_{-\infty}^{\infty}\exp\left[\frac{i\pi D_1}{\lambda B_1}\left(x^2+y^2\right)\right]\\&\times\exp\left[\frac{-i2\pi}{\lambda B_1}\left(\xi_o x+\eta_o y\right)\right]\\&\times P(x,y)\exp\left[\frac{i\pi A_2}{\lambda B_2}\left(x^2+y^2\right)\right]\\&\times\exp\left[\frac{-i2\pi}{\lambda B_2}\left(xu+yv\right)\right]\mathrm{d}x\mathrm{d}y\\=&\frac{e^{ikL_0}}{i\lambda B_2}\frac{1}{i\lambda B_1}\exp\left[\frac{i\pi D_2}{\lambda B_2}\left(u^2+v^2\right)\right]\\&\times\exp\left[\frac{i\pi A_1}{\lambda B_1}\left(\xi_o^2+\eta_o^2\right)\right]\iint_{-\infty}^{\infty}P(x,y)\\&\times\exp\left[\frac{i\pi}{\lambda}\left(\frac{D_1}{B_1}+\frac{A_2}{B_2}\right)\left(x^2+y^2\right)\right]\\&\times\exp\left\{\frac{-i2\pi}{\lambda}\left[\left(\frac{\xi_o}{B_1}+\frac{u}{B_2}\right)x\right.\right.\\&\left.\left.+\left(\frac{\eta_o}{B_1}+\frac{v}{B_2}\right)y\right]\right\}\mathrm{d}x\mathrm{d}y,\end{aligned} \tag{23}$$

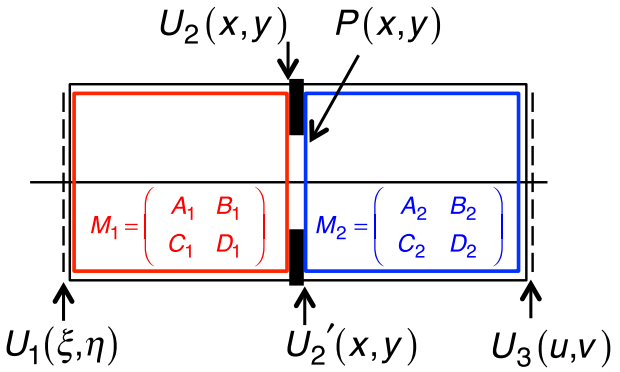

Fig. 5. Imaging with an aperture stop having amplitude transmittance P. First, propagate through an ABCD subsystem having matrix M_1, then multiply by the transmittance of the aperture stop, and then propagate with another ABCD subsystem having matrix M_2.

where L_0 is the axial optical path of the total system. This shows the relationship between the field in the output plane (whether an image plane or not) and the point source in the input plane.

The ABCD matrix for the total system (ignoring the aperture stop) is given by

$$M_T = M_2 M_1 = \begin{pmatrix} A_2 & B_2 \\ C_2 & D_2 \end{pmatrix} \begin{pmatrix} A_1 & B_1 \\ C_1 & D_1 \end{pmatrix} = \begin{pmatrix} A_2A_1 + B_2C_1 & A_2B_1 + B_2D_1 \\ C_2A_1 + D_2C_1 & C_2B_1 + D_2D_1 \end{pmatrix} = \begin{pmatrix} A_T & B_T \\ C_T & D_T \end{pmatrix}. \tag{24}$$

The condition that the total system is an imaging system is that $B_T = 0$,

$$B_T = A_2B_1 + B_2D_1 = 0, \quad \text{or} \quad \frac{D_1}{B_1} + \frac{A_2}{B_2} = 0. \tag{25}$$

After inserting this expression into the integrand above, the quadratic phase within the integral disappears, and we have

$$h(u, v; \xi_o, \eta_o) = \frac{e^{ikL_0}}{i\lambda B_2} \frac{1}{i\lambda B_1} \exp\left[\frac{i\pi D_2}{\lambda B_2}\left(u^2 + v^2\right)\right] \times \exp\left[\frac{i\pi A_1}{\lambda B_1}\left(\xi_o^2 + \eta_o^2\right)\right] \iint_{-\infty}^{\infty} P(x, y) \times \exp\left\{\frac{-i2\pi}{\lambda}\left[\left(\frac{\xi_o}{B_1} + \frac{u}{B_2}\right)x + \left(\frac{\eta_o}{B_1} + \frac{v}{B_2}\right)y\right]\right\} \mathrm{d}x\mathrm{d}y, \tag{26}$$

which is the image field from a delta function in the input plane at (ξ_o, η_o). This equation contains a Fourier transform of the aperture-stop transmittance function, evaluated at

$$f_x = \left(\frac{\xi_o}{\lambda B_1} + \frac{u}{\lambda B_2}\right) \quad \text{and} \quad f_y = \left(\frac{\eta_o}{\lambda B_1} + \frac{v}{\lambda B_2}\right). \tag{27}$$

Note the similarity of this equation with Eqs. (6–33) and (6–36) in [5].

The magnification of the imaging system is given by $A_T = A_2A_1 + B_2C_1$. Using the fact that the determinant of any ABCD matrix is unity, $A_1D_1 - B_1C_1 = 1$, or $C_1 = (A_1D_1 - 1)/B_1$, giving

$$M = A_T = A_2A_1 + B_2\frac{A_1D_1 - 1}{B_1} = A_2A_1 + \frac{B_2A_1D_1}{B_1} - \frac{B_2}{B_1}. \tag{28}$$

Furthermore, from above, $B_T = A_2B_1 + B_2D_1 = 0$, or $D_1 = -A_2B_1/B_2$, giving

$$M = A_T = A_2A_1 + \frac{B_2A_1}{B_1}\left(-\frac{A_2B_1}{B_2}\right) - \frac{B_2}{B_1} = A_2A_1 - A_2A_1 - \frac{B_2}{B_1} = -\frac{B_2}{B_1}, \tag{29}$$

a simple expression for the system magnification in terms of the ratio of the B components of the two matrices. Taking B_2 outside the brackets in Eq. (26) and using the expressions for M above, the impulse response becomes

$$h(u, v; \xi_o, \eta_o) = \frac{e^{ikL_0}}{i\lambda B_2} \frac{1}{i\lambda B_1} \exp\left[\frac{i\pi D_2}{\lambda B_2}\left(u^2 + v^2\right)\right] \times \exp\left[\frac{i\pi A_1}{\lambda B_1}\left(\xi_o^2 + \eta_o^2\right)\right] \iint_{-\infty}^{\infty} P(x, y) \times \exp\left\{\frac{-i2\pi}{\lambda B_2}\left[(u - M\xi_o)\,x + (v - M\eta_o)\,y\right]\right\} \mathrm{d}x\mathrm{d}y. \tag{30}$$

As in [5] (Sect. 6.3.3), defining normalized input-plane coordinates $\tilde{\xi} = M\xi$ and $\tilde{\eta} = M\eta$ and inserting Eq. (30) into Eq. (21) gives

$$h\left(u, v; \tilde{\xi}_o, \tilde{\eta}_o\right) = \frac{e^{ikL_0}}{i\lambda B_2} \frac{1}{i\lambda B_1} \exp\left[\frac{i\pi D_2}{\lambda B_2}\left(u^2 + v^2\right)\right] \times \exp\left[\frac{i\pi A_1}{\lambda M^2 B_1}\left(\tilde{\xi}_o^2 + \tilde{\eta}_o^2\right)\right] \iint_{-\infty}^{\infty} P(x, y) \times \exp\left\{\frac{-i2\pi}{\lambda B_2}\left[\left(u - \tilde{\xi}_o\right)x + (v - \tilde{\eta}_o)\,y\right]\right\} \mathrm{d}x\mathrm{d}y. \tag{31}$$

This is a generalization of [5], Eq. (6–33). Inserting this 4D function $h(u, v; \tilde{\xi}_o, \tilde{\eta}_o)$ into Eq. (21), integrating over normalized coordinates $(\tilde{\xi}, \tilde{\eta})$, and defining the ideal image as

$$U_g(\tilde{\xi}, \tilde{\eta}) = \frac{1}{|M|} U_1\left(\frac{\tilde{\xi}}{M}, \frac{\tilde{\eta}}{M}\right), \tag{32}$$

we obtain

$$U_3(u, v) = \exp\left[\frac{i\pi D_2}{\lambda B_2}\left(u^2 + v^2\right)\right] \iint_{-\infty}^{\infty} \left\{U_g\left(\tilde{\xi}, \tilde{\eta}\right) \times \exp\left[\frac{i\pi A_1}{\lambda M^2 B_1}\left(\tilde{\xi}^2 + \tilde{\eta}^2\right)\right]\right\} h\left(u - \tilde{\xi}, v - \tilde{\eta}\right) \mathrm{d}\tilde{\xi}\mathrm{d}\tilde{\eta}, \tag{33}$$

where the 2D (space-invariant) impulse response, h, is given by the Fourier transform of the aperture-stop transmittance,

$$h(u, v) = \frac{-e^{ikL_0}}{\lambda^2 B_2^2} \iint_{-\infty}^{\infty} P(x, y) \exp\left[\frac{-i2\pi}{\lambda B_2}(ux + vy)\right] \mathrm{d}x\mathrm{d}y. \tag{34}$$

This result is analogous to Eq. (6–42) in [5] if one does not discard the constant pure-phase term $-\exp(ikL_{01})$ and the two quadratic-phase exponentials and generalizes them to an arbitrary ABCD imaging system. Note that the 2D impulse response, $h(u, v)$, does not convolve just the field in the input plane but convolves the product of the field in the input plane

with an extra quadratic-phase exponential. The resulting convolution is multiplied by a second quadratic-phase exponential in the output plane coordinates. These extra quadratic-phase exponentials get canceled for the case of incoherent imaging (where they can be ignored) but not for coherent imaging where the phases in the input and output planes matter, except for special cases, described in Sect. 6.3.2 and Problem 6-12 in [5]. For example, the internal quadratic-phase exponential can be taken outside the integral if it varies little over the width of the impulse response, $h(u, v)$. Note that the ABCD imaging equations, Eqs. (33) and (34), are not quite space-invariant, but the image field is nevertheless a convolution of the 2-D impulse response with that product of the ideal image field with a quadratic-phase exponential.

A. Location of the Exit Pupil

For imaging, the impulse response given in Eq. (34) is a Fourier transform of the aperture stop with spatial frequencies $f_x = u/(\lambda B_2)$, whose scale depends only on the part of the system following the aperture stop. Ordinarily, for imaging, we consider the impulse response to be the Fourier transform not of the aperture stop (although it is that) but of the exit pupil of the system. The exit pupil is an image of the aperture stop as seen through the intervening optics between the aperture stop and the image plane. To determine where the exit pupil (the image of P) is located, consider that the ABCD matrix from the aperture stop to the exit pupil would be the second ABCD matrix, taking us to the image plane, followed by the free-space propagation from the image plane to the exit pupil, which distance we will call d, which we wish to determine. That gives us the ABCD matrix from the aperture stop to the exit pupil as

$$M_{\text{sep}} = \begin{pmatrix} 1 & d \\ 0 & 1 \end{pmatrix} \begin{pmatrix} A_2 & B_2 \\ C_2 & D_2 \end{pmatrix} = \begin{pmatrix} A_2 + dC_2 & B_2 + dD_2 \\ C_2 & D_2 \end{pmatrix} = \begin{pmatrix} A_{\text{sep}} & B_{\text{sep}} \\ C_{\text{sep}} & D_{\text{sep}} \end{pmatrix}. \quad (35)$$

Because going from the plane of the aperture stop to the plane of the exit pupil should be an imaging condition, with $B_{\text{sep}} = 0$, we have $B_2 + dD_2 = 0$ or $d = -B_2/D_2$.

The magnification of the exit pupil relative to the aperture stop is given by

$$A_{\text{sep}} = A_2 + dC_2 = A_2 - \frac{B_2}{D_2} C_2 = \frac{A_2 D_2 - B_2 C_2}{D_2} = \frac{1}{D_2}, \quad (36)$$

giving

$$-d = B_2/D_2 = A_{\text{sep}} B_2, \quad (37)$$

which is the distance from the exit pupil to the image plane.

If the diameter of the aperture stop is D_p, then the diameter of the exit pupil is $D_{\text{ep}} = A_{\text{sep}} D_p$, and the (paraxial) angular subtense of the exit pupil, as seen from the image plane, is

$$\frac{A_{\text{sep}} D_p}{-d} = \frac{A_{\text{sep}} D_p}{A_{\text{sep}} B_2} = \frac{D_p}{B_2}, \quad (38)$$

which is the same as the diameter of the pupil stop divided by the effective focal length B_2, of the second half of the system. That is, the angular subtense of the exit pupil, as seen from the image, is equal to the ratio of the diameter of the exit pupil $A_{\text{sep}} D_p$ to the distance from the exit pupil to the image $-d = A_{\text{sep}} B_2$, and that is the same ratio as the physical diameter of the pupil stop D_p divided by the effective focal length B_2 of the second half of the imaging system. Thus, both methods predict the same diffraction effects affecting the impulse response h given by the Fourier transform of either the aperture stop or the exit pupil. This can also be seen by employing a change of variables $x_{\text{ep}} = A_{\text{sep}} x$ in Eq. (34) and using

$$P_{\text{ep}}(x, y) = P\left(x/A_{\text{sep}}, y/A_{\text{sep}}\right) \quad \text{and}$$
$$P(x, y) = P_{\text{ep}}\left(A_{\text{sep}} x, A_{\text{sep}} y\right), \quad (39)$$

giving

$$h(u, v) = \frac{-e^{ikL_0}}{\lambda^2 \left(A_{\text{sep}} B_2\right)^2} \iint_{-\infty}^{\infty} P_{\text{ep}}\left(x_{\text{ep}}, y_{\text{ep}}\right) \times \exp\left[\frac{-i2\pi}{\lambda\left(A_{\text{sep}} B_2\right)}\left(u x_{\text{ep}} + v y_{\text{ep}}\right)\right] \mathrm{d}x_{\text{ep}} \mathrm{d}y_{\text{ep}}, \quad (40)$$

which explicitly shows that propagation from the exit pupil to the image plane, a distance of $-d = A_{\text{sep}} B_2$ away, gives the identical impulse response as propagation from the aperture stop to the image plane. The image-plane Rayleigh two-point resolution criterion [5] for an ABCD imaging system having a circular aperture is 1.22 λF#, where the f-number is given by the ratio $\text{F\#} = D_p/B_2 = D_{\text{ep}}/(A_{\text{sep}} B_2)$, that is, the ratio of the aperture-stop diameter to the effective focal length of the system is equal to the ratio of the exit-pupil diameter to the distance from the exit pupil to the image plane.

8. DIGITAL COMPUTATION OF PROPAGATIONS

When performing numerical ABCD propagations using a computer, one works with discrete samples of the field and discrete Fourier transforms (DFTs) instead of the continuous fields and integrals discussed so far. Often the fast Fourier transform (FFT) approach to compute the DFTs is used, since it is typically many times faster than the DFT. This choice results in a particular relationship between the output-plane sample spacings and the input-plane sample spacings that in some scenarios are unfavorable. More flexible sample spacings can be obtained by using approaches, such as the matrix triple product, the chirp-Z transform [12], and the scalable angular spectrum ([13,14], Sect. 6.4). For simplicity, in this paper we only address the single-FT and double-FT versions using FFTs. Ordinarily, when performing a DFT or FFT to compute a Fresnel or Fraunhofer propagation integral, we compare a sampled version of the Fourier kernel of the integral with the kernel of the DFT, and we arrive at the relationship between the output sample spacing δ_2 and the input sample spacing δ_1. In the case of the single-FT ABCD propagation given in Eq. (7), this gives

$$\delta_2 = \lambda B/(N\delta_1), \quad (41)$$

for an $N \times N$ FFT [15]. In contrast, in the double-FT version of ABCD propagation, which is computed using multiplication with a transfer function in the Fourier domain, as given by Eq. (12), we obtain the same sample spacing in the output plane as the input plane: $\delta_2 = \delta_1$. Because the inputs to and outputs from an FFT have the same linear number of pixels N, scaling of the sample spacings likewise scales the physical width $N\delta_i$ of the field in the computational window. Therefore, selecting the discrete form of either the single-FT or the double-FT versions of the ABCD propagation will largely depend on the relative widths desired of the input and output fields. If they are comparable in width (e.g., propagating a plane wave forward a short distance or having a propagation Fresnel number much greater than, say, 10 or 50), then the double-FT version will typically be more efficient. On the other hand, if they differ greatly in width (e.g., propagating from a pupil plane to an image plane or propagating from the near field to the far field), then the single-FT version will typically be more efficient. If the less efficient method is chosen, then one finds that it is necessary to embed the arrays in larger arrays of zeros to avoid aliasing, thereby driving up both the computational cost and memory requirements.

Aliasing occurs in the computations when the propagated field extends laterally beyond the physical width of the computational window, and energy wraps around from one edge of the array to the opposite edge. If the field has passed through an aperture with hard edges, then the Fourier transform of that field will certainly be aliased because it extends out to infinity, but that aliasing can be minimized by representing the field by a large array of numbers in the computer. Another source of aliasing is due to phase terms within the propagation integral itself, which we analyze here. One way to appreciate this is to note that if one samples a tilted plane wave such that the linear phase changes by 2π from one sample to the next, then that tilted plane wave is indistinguishable from an on-axis plane wave, since $\exp(i\,2\pi) = \exp(i\,0) = 1$. According to the Fourier shift theorem [5], a linear phase in one domain results in a proportional translation in the other domain. For a length-N FFT of a linear-phase exponential having the phase change of 2π per sample, the transform is shifted by exactly N samples. It has translated off one edge of the computational window, wrapped around to the opposite edge, and has returned back to its original position. Proportionally, if the linear-phase exponential has a phase that changes by π per sample, then it translates by $N/2$ samples, that is, by half of the computational window. Hence we will have very substantial aliasing when the local slope of the quadratic-phase exponential inside the integral of Eq. (7) is π per sample or greater. Assume an input-plane aperture of width $D_{\text{ap}} = M\delta_1$, where M is the number of samples across the width of the aperture. This aliasing condition can be calculated by using the concept of the local spatial frequency [5], taking the partial derivative of the quadratic phase with respect to a transverse coordinate and multiplying that by the sample spacing, and having that product be greater than or equal to π at the edge of the aperture, at $D_{\text{ap}}/2$, at pixel $M/2$. One can alternatively compute the phase at the last sample within the aperture, at $M/2$ from the origin minus the phase at $(M/2-1)$ from the origin, and having that difference be greater than or equal to π. By applying the first approach to the quadratic phase term in Eq. (7), we have

$$\delta_1 \frac{\partial}{\partial \xi} \frac{\pi A}{\lambda B} \left(\xi^2 + \eta^2\right)\Big|_{\xi = D_{\text{ap}}/2} = \frac{D_{\text{ap}}}{M} \frac{2\pi A}{\lambda B} \frac{D_{\text{ap}}}{2} = \frac{4\pi A N_F}{M} \le \pi, \tag{42}$$

or, to avoid this aliasing, we need

$$M \ge 4AN_F, \tag{43}$$

where

$$N_F = \frac{D_{\text{ap}}^2}{4\lambda B}, \tag{44}$$

is the Fresnel number for the propagation, which is the number of π of the phase change of the quadratic phase from the center to the edge of the aperture. Eq. (5–12) in [5] is a special case of Eq. (43) for the case of free-space propagation. For a short-distance propagation of a roughly collimated field $U_1(\xi, \eta)$, Eq. (43) can require an overly burdensome number of pixels across the aperture to avoid aliasing by the quadratic phase inside the integral of Eq. (7). If, on the other hand, $U_1(\xi, \eta)$ contains a converging or diverging quadratic-phase exponential, then the phase of the exponential should be added to the quadratic phase explicit in the integral in Eq. (7) to determine when aliasing occurs due to quadratic-phase terms.

If instead one employs the double-FT, Fourier-domain convolutional form of ABCD propagation, given in Eq. (12), then the maximum slope of its quadratic phase must be analyzed. First, the sample spacing for the FFT in the Fourier domain is $\delta_f = 1/(N\delta_1)$, where $N\delta_1$ is the width of the computational window in the input plane (which may include some zero padding, with $N \ge M$), and the width of the computed Fourier domain is $N\delta_f = 1/\delta_1$. Then, we need

$$\begin{aligned} &\delta_f \frac{\partial}{\partial f_x} \frac{\pi\lambda B}{A} \left(f_x^2 + f_y^2\right)\Big|_{f_x = 1/(2\delta_1)} \\ &= \frac{1}{N\delta_1} \frac{2\pi\lambda B}{A} \frac{1}{2\delta_1} = \frac{\pi\lambda B}{AN\delta_1^2} \le \pi, \end{aligned} \tag{45}$$

or

$$N \ge \frac{\lambda B}{A\delta_1^2}, \tag{46}$$

which can be a burdensome number of samples for large B, for example, long propagation distances, or for an overly fine sample spacing δ_1. Consequently, one would benefit from choosing Eq. (7) or Eq. (12), depending on the value of B, which is in the numerator in Eq. (7) and in the denominator in Eq. (12). A further factor in favor of the double-FT Eq. (12) is that violating the aliasing condition of Eq. (46) often produces only a small amount of aliased energy compared to violating the aliasing condition of Eq. (43) for the single-FT propagation in Eq. (7). This occurs when the Fourier transform of $U_1(\xi, \eta)$ drops off a great deal with higher spatial frequencies, which is usually the case, for example, for an aperture illuminated by a plane wave. Then, the location of the maximum slope of the phase causing the aliasing is where the Fourier transform of $U_1(\xi, \eta)$ has a small value. Thus, little energy is aliased. However, we often have situations in which the quadratic phase in the integral of the single-FT Eq. (7) has a maximum slope near the edge of an aperture, and if the aperture is uniformly illuminated,

then $U_1(\xi, \eta)$ would have a large value in those locations, and a large amount of energy would be aliased. Hence, the aliasing condition for the single-FT Eq. (7) is often much stricter than the aliasing condition for the double-FT Eq. (12). An exception is the case of propagating a laser speckle field, for which the Fourier transform of $U_1(\xi, \eta)$ will typically have large values at higher spatial frequencies. In that case, the aliasing condition for Eq. (12) must be taken strictly. Issues surrounding sampling and aliasing can be complicated, and the reader may find further discussions in [5,14,16].

In the discussion of aliasing above, we concentrated on the quadratic-phase exponentials inside the integrals. It also easily happens that the quadratic-phase exponentials outside the integrals can be undersampled as well. These include the phase proportional to D/B in Eq. (7), the phase proportional to C/A in Eq. (11), and the phase proportional to D_2/B_2 in Eq. (33). When the final phase does not matter, these can be ignored, but when interfering the field with another field or if further propagations are required, then the fidelity of those external quadratic phases matters. In that case it can be advantageous to keep track of that quadratic phase separately, saving its quadratic coefficient rather than evaluating the exponential. Then, if further propagation is required, one can add the saved quadratic-phase coefficient to the quadratic-phase coefficient within the next ABCD integral for the next propagation, and numerically evaluate that net quadratic-phase exponential. Aliasing due to quadratic-phase exponentials would then be driven by that net quadratic-phase exponential rather than just by the one given in the expression for the ABCD propagation.

Finally, reduced computational burdens can sometimes also be achieved by first propagating from the input plane to a second plane, where aliasing is minimized and small array sizes can be used, and then propagating from that plane to the desired output plane {[15], after Eq. (3.6)}.

Further references on numerical propagations are given in [17,18].

9. SUMMARY AND REMARKS

The ABCD (ray-transfer) method of analyzing paraxial optical systems was originally developed for paraxial geometrical optics and was then shown by Collins to be applicable to wave-optics paraxial propagation calculations as well. It can be expressed in two ways. The first version is a single Fourier integral, the single-FT version, with quadratic-phase exponentials inside and outside the integral, which has the Fresnel propagation integral as a special case for free-space propagation. The second version is where the propagation integral is expressed as a convolution integral with the ABCD-propagation impulse response, which is in the form of a quadratic-phase exponential. This second version, the double-FT version, can be expressed in the Fourier domain as a product with the ABCD-propagation transfer function, which is also in the form of a quadratic-phase exponential. It takes two Fourier transforms to compute and has the free-space paraxial angular spectrum propagation, which is equivalent to the Fourier-domain version of the Fresnel propagation, as a special case. Which of these two versions is more accurate and computationally efficient depends on the relative widths of the desired input plane and output plane regions of interest, with the double-FT version favoring similar widths and the single-FT version favoring greatly differing widths. It also depends on the ABCD Fresnel number, given by the square of the input-plane aperture diameter (when there is one) divided by $4\lambda B$, with the double-FT version favoring larger values (e.g., 10 or 50 or greater) of the Fresnel number and the single-FT version favoring smaller values (e.g., 50 or 10 or smaller). Performed numerically, both types of propagations can result in aliasing, and the effects of aliasing can be worse for the single-FT version than for the double-FT version when aliasing occurs. In some cases it is computationally advantageous to perform two propagations, the first from the input plane to an advantageous plane, and the second from that plane to the desired plane.

In the case of an imaging system, for which $B = 0$, ABCD propagation predicts a perfect image. To include diffraction effects, one must perform a first ABCD propagation from the object plane to the aperture stop within the imaging system, multiply by the transmittance function of the aperture stop, and then ABCD propagate from the aperture stop to the image plane. This was shown to be equivalent to the convolution of the product of the ideal image of the field in the object plane with an object-domain quadratic-phase exponential with the ABCD impulse response, given in Eqs. (33) and (34). This makes imaging of coherent fields not quite space-invariant. That impulse response is given by the Fourier transform of the aperture stop transmittance function over an effective focal length of B_2, the B coefficient of the ABCD matrix going from the aperture stop to the image plane. One can alternatively calculate the location of the exit pupil relative to the image plane and calculate the ABCD impulse response as a Fourier transform from the exit pupil to the image plane, with a propagation distance of B_2/D_2.

When imaging optical fields, additional quadratic phase exponentials naturally occur in the object and image planes, and these need to be included in the propagations. The quadratic phases do, however, go away when one is imaging an incoherent object, in which case one convolves the object intensity distribution with the point-spread function $|h|^2$, which is the squared magnitude of the coherent impulse response analyzed here. The optical transfer function would then be the Fourier transform of $|h|^2$. For light at the object that is partially coherent, one can compute the image intensity using a 4D integral involving conjugate products of two differently shifted versions of h {[5], Eq. (7–8)} or more generally can compute the propagation of the mutual intensity function from an input plane to an output plane with a similar 4D integral {[6], Eq. (7.154)}.

Since fractional Fourier transforms and linear canonical transforms are special cases of ABCD propagation integrals, these results, with appropriate change of parameters, can be used for them as well. Those two formalisms are often used for an interesting phase-space interpretation [6,7] of propagating fields, which includes the Fourier transform being a rotation in phase space by 90°.

The propagation of optical fields through complicated optical systems is greatly simplified by the use of ABCD propagation integrals, as it can be accomplished with only one or two Fourier transforms rather than with the many transforms that would be needed if one were to propagate from one lens element to the next through such a system.

Disclosures. The author declares no conflicts of interest. There was no funding involved with this research.

Data availability. No data were generated or analyzed in the presented research.

REFERENCES

1. S. A. Collins, "Lens-system diffraction integral written in terms of matrix optics," J. Opt. Soc. Am. **60**, 1168–1177 (1970).
2. A. E. Siegman, *Lasers* (University Science, 1986), Chaps. 15 and 20.
3. E. Hecht, *Optics*, 5th ed. (Pearson, 2017), Sect. 6.2.1.
4. M. Born and E. Wolf, *Principles of Optics*, 7th ed. (Cambridge University, 1999).
5. J. W. Goodman, *Introduction to Fourier Optics*, 4th ed. (W.H. Freeman and Co., 2017), Sections 4.2.6, 6.4 and B.3.
6. H. M. Ozaktas, Z. Zalevsky, and M. A. Kutay, *The Fractional Fourier Transform with Applications in Optics and Signal Processing* (Wiley, 2001).
7. J. J. Healy, M. A. Kutay, and H. M. Ozaktas, eds., *Linear Canonical Transforms: Theory and Applications* (Springer, 2016).
8. F. S. Oktem and H. M. Ozaktas, "Equivalence of linear canonical transform domains to fractional Fourier domains and the bicanonical width product: a generalization of the space–bandwidth product," J. Opt. Soc. Am. A **27**, 1885–1895 (2010).
9. H. T. Yura and S. G. Hanson, "Optical beam wave propagation through complex optical systems," J. Opt. Soc. Am. A **4**, 1931–1948 (1987).
10. S. G. Hanson, M. L. Jakobsen, and H. T. Yura, "Complex-valued ABCD matrices and speckle metrology," in *Linear Canonical Transforms: Theory and Applications*, J. J. Healy, M. A. Kutay, and H. M. Ozaktas, eds. (Springer, 2016), pp. 397–428.
11. S. A. Collins and M. Zabel, "Ray matrices, transfer functions, and intensities," in *OSA Annual Meeting* (Optica Publishing Group, 1989), paper WN5.
12. A. S. Jurling, M. D. Bergkoetter, and J. R. Fienup, "Techniques for arbitrary sampling in two-dimensional Fourier transforms," J. Opt. Soc. Am. A **35**, 1784–1796 (2018).
13. E. A. Sziklas and A. E. Siegman, "Diffraction calculations using fast Fourier transform methods," Proc. IEEE **62**, 410–412 (1974).
14. J. D. Schmidt, *Numerical Simulations of Optical Wave Propagation, With Examples in MATLAB* (SPIE, 2010).
15. J. R. Fienup, J. C. Marron, T. J. Schulz, *et al.*, "Hubble space telescope characterized by using phase retrieval algorithms," Appl. Opt. **32**, 1747–1767 (1993).
16. D. G. Voelz, *Computational Fourier Optics, a MATLAB Tutorial* (SPIE, 2011), vol. **TT89**.
17. B. M. Hennelly and J. T. Sheridan, "Generalizing, optimizing, and inventing numerical algorithms for the fractional Fourier, Fresnel, and linear canonical transforms," J. Opt. Soc. Am. A **22**, 917–927 (2005).
18. B. M. Hennelly and J. T. Sheridan, "Fast numerical algorithm for the linear canonical transform," J. Opt. Soc. Am. A **22**, 928–937 (2005).